Control of tuned masses using MR dampers and a new real time feedback signal and physical controller

R. Zemp
Pontificia Universidad Católica de Chile

J. C. de la Llera
Pontificia Universidad Católica de Chile

F. Weber
Empa, Swiss Federal Laboratories for Materials Science and Technology

SUMMARY:
A scaled prototype of an MR damper was active in passive mode on a 160 ton tuned mass in a 21-story building in Santiago, Chile, during the February 27, 2010 earthquake. More recently, a full scale ±100 cm stroke MR damper was designed, manufactured, and is being tested for the same building. The implementation considers a new real time structural measurement system developed to acquire building displacements as feedback for the physical controller of the TM-MR damper assembly. The new measurement system was successfully tested on a shaking table model at Empa. Moreover, results from a number of nonlinear simulations on the building with the full scale semi-active damper shows that the mean displacement reduction for the setup considered is 22% more effective than the building with the bare tuned masses. Finally, the solution was identified to be fairly cost-effective as compared with a passive solution or the bare case.

Keywords: MR dampers, earthquake response, physical controller, real time structural measurement (RTSM)

1. INTRODUCTION

A scaled magneto-rheological (MR) damper was implemented in one of two 160 ton tuned masses (TM) placed at the roof of a 21-story building (PA) in Santiago in Chile in 2008 (Zemp et al. 2008). The building underwent the strong motions induced by the M_w 8.8 earthquake on February 27, 2010. The building sustained the motions with no structural or non-structural damage, and remained fully operative after the earthquake. Since the damper was a scaled-down proof-of-concept device, it was designed to a limited maximum stroke of ±10 cm and nominal force capacity of 150 kN. The device was as a proof-of-concept damper, and was connected to a single mass through a sacrificial system intended to shear-off, as it did, as the displacement of the mass exceeded the stroke of the damper.

The structural concept of the RC building includes two TM in opposite sides of the plan designed to control both, the fundamental transversal and rotational modes (Zemp et al. 2008) and, hence, the maximum displacement demand at both building edges. The 150 kN proof-of-concept MR damper was designed, manufactured, dynamically tested, and finally implemented as part of a previous research (Zemp et al. 2011a, 2011b) intended to: (i) test integrally and in real conditions a new physical controller, and (ii) test all aspects of this proof-of-concept MR device and its practical implementation. Once concluded, the MR damper was left in passive mode in the building as it worked during the 2010 earthquake.

This small scale application adds to several real-scale applications of MR dampers on built structures. The first full-scale application of an MR damper dates from 2001, as two 300 kN MR dampers were installed at the Tokyo National Museum of Emerging Science and Innovation (Spencer and Nagarajaiah. 2003). In residential structures, a 400 kN MR damper is working in conjunction with base isolation in a Japanese building (Fujitani et al. 2003). MR dampers are also used to control cable vibrations in cable-stayed bridges, such as in the Dongting Lake Bridge in Hunan in China (Spencer and Nagarajaiah. 2003) and the Dubrovnik Bridge in Croatia (Weber et al. 2006).

The literature on MR dampers is quite vast and there are significant contributions in terms of the dynamic response of structures with these devices (Lee et al. 2008; Lin et al. 2005), their modelling and control (Dyke and Spencer. 1996), and their design and testing (Yang. 2001). An MR damper represents a controllable smart collection of infinite viscous dampers within a range of capacity, and naturally, due to the fluid and electronics their cost ends up being higher than viscous dampers. Viscous dampers are always in direct competition with the MR solution in technical as well as economic terms.

This article summarizes some of the results of a second phase of this MR initiative at the PA building and expands on the earlier work by developing and implementing a new real-scale MR damper with ±100 cm stroke and capacity of 400 kN to control one of the two 160 ton TMs. The design, manufacturing, testing, and control of such damper in a real-life situation has several technical complications that are described herein and need to be overcome before it can be implemented. The new damper is already manufactured and is being dynamically tested, through an interesting procedure described next. The physical controller of the semi active MR device needs real time information about the building during an earthquake. A new real time structural measurement, its scaled shaking table test, results of numerical simulations of the performance of the TM-MR damper assembly and an evaluation of the cost efficiency of the MR damper case are shown as well.

2. PRE-EARTHQUAKE TM-MR DAMPER SOLUTION

Shown in Fig. 2.1 are a schematic view of the reinforced concrete building and a photography of the proof-of-concept MR damper installed in 2008. The damper had a stroke of ±10 cm and was connected to the tuned mass at the flexible building edge (Fig. 2.1). The tuned masses installed on the top floor of the building were designed to reduce structural vibrations mainly in the flexible (transverse) Y-direction of the building, as well as the rotational motions of the plan.

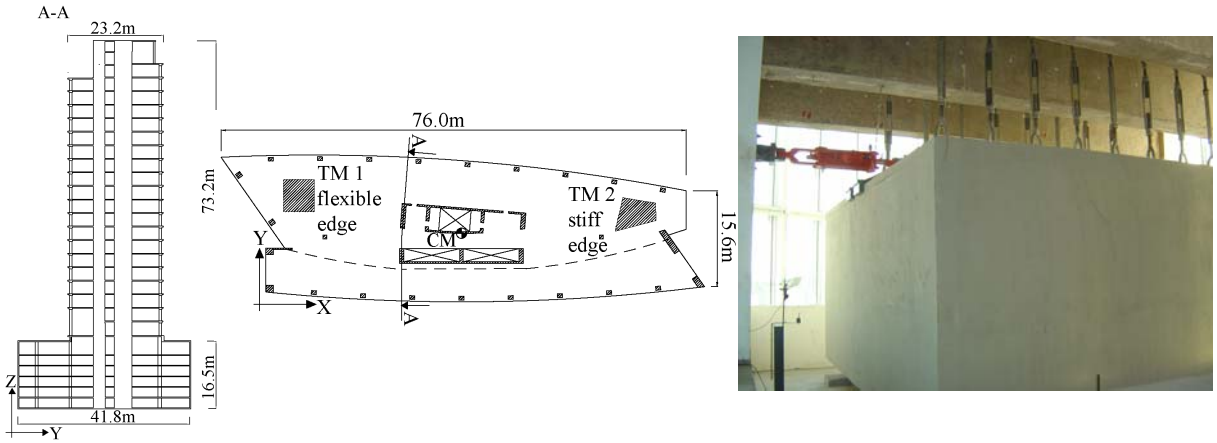

Figure 2.1. Building setup with TM and proof-of-concept MR damper on the flexible edge TM in Y-direction

The nominal and measured dynamic properties of the building are summarized in Table 2.1 (Zemp et al. 2011a). As it is shown, the nominal periods predicted by a structural model of the building are between 3% up to 28% higher than the periods measured by micro-vibration prior to the earthquake. Due to cracking and plastic deformations of the RC structure, the periods of the building tend to increase during strong motion. Therefore, for numerical simulations of the building with TMs and MR dampers, the two sets of periods are taken as representative limits for the non-cracked and cracked conditions. The measured damping ratios of different structural building modes obtained by micro-vibration vary between 0.8% and 1.7%. Furthermore, the 160 ton TMs have an uncoupled period of 2.7s and measured damping ratio ranging between 0.1 and 0.25%. Because the implemented TMs are supposed to be tuned to the nominal set of periods, the (uncracked) measured period is not tuned, as it is for the nominal case.

Table 2.1. Vibration periods and damping ratios of building PA determined by micro vibrations

MODE		Nominal period	Measured period	Period ratio	Damping ratio
N°	Direction	(s)	(s)		ξ_s (%)
1	Y	2.68	2.10	1.276	1.6
1	θ	2.01	1.67	1.204	1.7
1	X	1.30	1.12	1.161	1.1
2	Y	0.69	0.60	1.150	0.8
2	θ	0.58	0.54	1.074	1.0
3	Y	0.33	0.27	1.222	-
2	X	0.31	0.30	1.033	-

The equations of motion that govern the dynamic behaviour of the building with TM and dampers may be written as (Zemp et al. 2011a).

$$\begin{bmatrix} \widetilde{\mathbf{M}} + \mathbf{\Phi}^T\mathbf{L}^T\mathbf{mL}\mathbf{\Phi} & \mathbf{\Phi}^T\mathbf{L}^T\mathbf{m} \\ \mathbf{mL}\mathbf{\Phi} & \mathbf{m} \end{bmatrix} \begin{bmatrix} \ddot{\boldsymbol{\eta}} \\ \ddot{\mathbf{p}} \end{bmatrix} + \begin{bmatrix} \widetilde{\mathbf{C}} & \mathbf{0} \\ \mathbf{0} & \mathbf{c} \end{bmatrix} \begin{bmatrix} \dot{\boldsymbol{\eta}} \\ \dot{\mathbf{p}} \end{bmatrix} + \begin{bmatrix} \widetilde{\mathbf{K}} & \mathbf{0} \\ \mathbf{0} & \mathbf{0} \end{bmatrix} \begin{bmatrix} \boldsymbol{\eta} \\ \mathbf{p} \end{bmatrix} + \begin{bmatrix} \mathbf{0} \\ \mathbf{F}_{TMD} \end{bmatrix} = -\begin{bmatrix} \mathbf{\Phi}^T\mathbf{Mr} + \mathbf{\Phi}^T\mathbf{L}^T\mathbf{mLr} \\ \mathbf{mLr_p} \end{bmatrix} \ddot{\mathbf{u}}_g \quad (2.1)$$

where $\boldsymbol{\eta}$ and $\mathbf{\Phi}$ are the Ritz coordinates and vectors for the first 20 modes of a total of 78 DOFs; $\mathbf{u} = \boldsymbol{\eta}\mathbf{\Phi}$ are the physical DOFs of the structure; $\widetilde{\mathbf{M}}$; $\widetilde{\mathbf{C}}$; $\widetilde{\mathbf{K}}$ are the mass, damping (classic) and stiffness matrices in modal coordinates; **M**, **C**, and **K** are the mass, damping, and stiffness matrices of the original structure; **r**, is the influence vector for earthquake excitation; $\ddot{\mathbf{u}}_g$ is the ground acceleration; **p** are the displacements of the TMs relative to the roof; **L** is the kinematic transformation matrix between the degrees of freedom **u** and the building displacements at the location of the TMs; **m** and **c** are the mass and the linear viscous damping matrices of TMs; $\mathbf{r_p}$ is the input influence vector of the TM for earthquake excitations; and $\mathbf{F}_{TMD}=[F_{1x}\ F_{1y}\ F_{2x}\ F_{2y}\ ]^T$ is the vector including all nonlinear terms in the equations of motion of each TM in physical coordinates **p**. The (*i, k*) element of this vector with i =1,2 and k=*x,y* subjected to a Y-direction ground motion is given by Eqn. 2.2 (Zemp et al. 2011a)..

$$F_{TMD,ik} = m_i \frac{\dot{p}_{ik}^2}{L_i^2 - p_{ik}^2} p_{ik} + m_i g \frac{\sqrt{L_i^2 - p_{ik}^2}}{L_i^2} p_{ik} + F_{MR(\tau,\dot{p},t)} \frac{L_i^2 - p_{ik}^2}{L_i^2} - c_i \frac{p_{ik}^2}{L_i^2} \dot{p}_{ik} - m_i \frac{p_{ik}^2}{L_i^2} \mathbf{L}(\mathbf{r}_{ip}\ddot{u}_{gy} + \mathbf{\Phi}\ddot{\boldsymbol{\eta}}) \quad (2.2)$$

where m is the mass of the TM; L is the free length of the hanging mass; g is the acceleration of gravity; $F_{MR(\tau,\dot{p},t)}$ is the horizontal MR damper force, which depends on the damper geometry, the damper velocity, and the shear strength τ in the MR fluid, which is introduced by the voltage source to follow a control strategy as presented next.

A new physical controller intended to reduce structural displacements was proposed and studied. Since an MR damper is a semi-active device, the sign of the damper force depends on the direction of the damper velocity. The different physical states of the structure and TM used to specify the control are presented for a single DOF model in Fig. 2.2 (Zemp et al. 2011a). In State 1a, as the building is displacing away from the equilibrium state, and the relative velocity between the structure and mass is negative, the MR damper engages with maximum capacity to try to stop the building leading to an on-state for the MR damper. However, if the relative velocity is positive as in State 1b, the mass is swinging away from the structure, and intuitively, the MR damper should apply its minimum damper force leading to an off-state of the MR damper. In State 2, when the building is returning to its equilibrium configuration, it is not obvious if it is better to push the structure back to the original position by applying maximum force, brake this return, or apply an intermediate damper force. Consequently, in State 2 different controllers were evaluated using these push-back forces (State 2a) and braking forces (State 2b) ranging from 0 to 100% intensity (Zemp et al. 2011a). This control strategy has the advantage that the control requires very few real time information of the structure and surprisingly, its performance is similar and sometimes better than conventional controllers. In the particular case of the control with push back forces (State 2a), only the sign of the first building mode

displacement and the sign of the damper force are required for the real-time control signals.

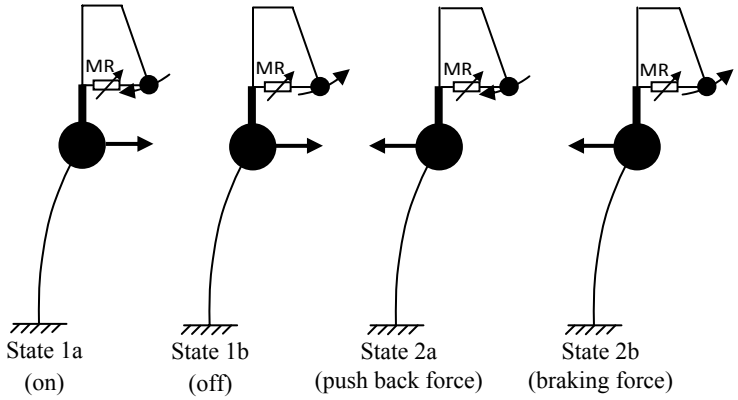

Figure 2.2. Schematic sketch of states of physical controller

A large number of analytical simulations of the building subjected to different Chilean and US ground motion records were developed in order to estimate the effectiveness of the TM-MR damper solution. These results are presented elsewhere (Zemp et al. 2011a). Simulation results for the new full-scale MR damper setup are discussed later.

A schematic internal view of the initial 150 kN MR damper developed is presented in Fig. 2.3. When the piston of the damper begins to move, the MR-fluid is forced to pass through an annular gap between chambers. Using two coils a magnetic flux can be applied which changes the state of the MR-fluid from liquid to semi-solid with a yield shear strength that depends on the current intensity (Bingham fluid). A critical aspect for the design phase of an MR damper is to confine the magnetic flux and minimize leakage of magnetic flow.

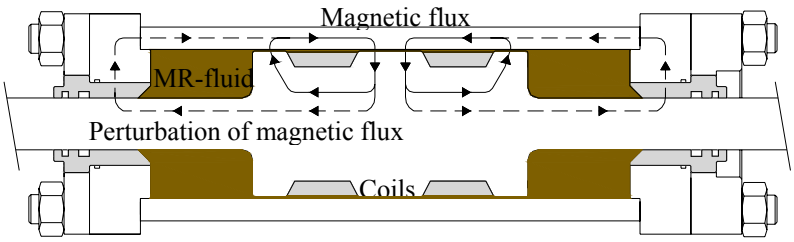

Figure 2.3. Scheme of 150kN damper section

A complete dynamic testing program for the ±10cm stroke prototype device was carried and included 68-cyclic as well as 50-hybrid simulation tests. With this thorough testing program, the MR damper design was validated, and the damper responded as expected with relatively low viscous force in its off-state, and with a maximal force of 150 kN for the on-state as current intensity was input into the two coils. The measured dynamic range of the damper, defined as the ratio between the maximum damper force in on- and off-state, was 16, which is excellent. For hybrid simulation tests, in which the MR damper was tested simultaneously with the numerical simulation of the building with TMs, led us to good results for the new physical controller.

A set of tests were also performed on the structure by attaching (or not) the MR damper to the TM. The setup of the implementation is presented in Fig. 2.4. Relative displacements between the TM and the structure, and absolute velocity of the 21st story floor, were both measured (Fig. 2.4a). The computer acquires these signals in real-time, and the controller applies the required voltage to the MR damper coils to drive the force according to the bang-bang control strategy implicit in the physical controller.

Pull-back tests were performed on the TM along the flexible edge. By pushing with a horizontal hydraulic jack, an initial displacement of -10 cm was applied to the mass (Fig. 2.4b). Pushing upward with another vertical jack, the system applying the horizontal force was buckled, and the mass released. Results with and without the MR damper connected to the mass are presented in Fig 2.5 (Zemp et al. 2011b). The left hand side of the Figure shows the relative displacement between the TM and the floor of the 21st story; the right hand side shows the total displacement of the same floor. The latter signal was obtained by integration of the measured velocity. Higher building displacements are observed as the MR damper is not connected to the mass. As the MR damper is in controlled mode, the building shows its best performance, which validates the idea behind the physical controller. In other tests, where we introduced into the control an artificial time delay, the observed building displacement for the on-sate of the MR damper was larger than the off-case. Because of that a maximum delay of about 0.07s was considered acceptable.

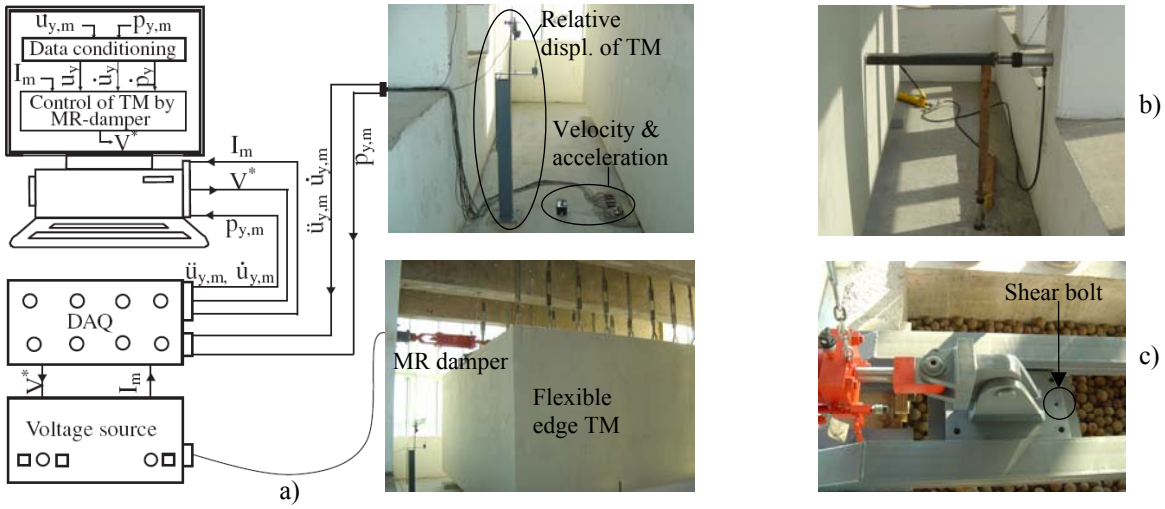

Figure 2.4. Implementation of the proof-of-concept MR damper: a) TM-MR damper assembly, b) pullback test setup, and c) MR damper connection to TM with shear-off system

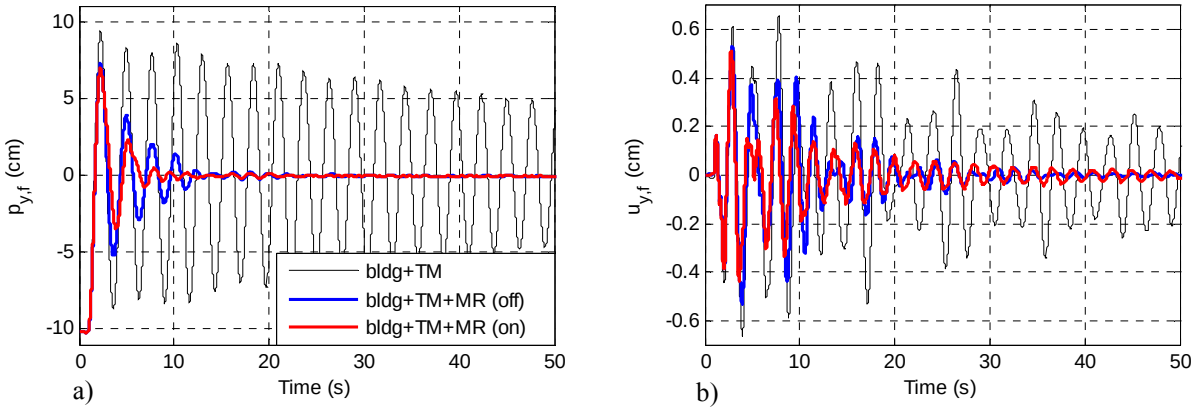

Figure 2.5 Results of pull back test: a) relative TM displacement, and b) total 21st floor displacement

3. NOMINAL PERFORMANCE OF THE MR DAMPER-TM DESIGN DURING THE EARTHQUAKE

As intended by design, the connection between the MR damper and the TM sheared-off during the February 27, 2010 earthquake, which implies that the TMs went well beyond the 10 cm displacement proposed for the scaled-down MR prototype. The connection between the MR damper and the mass was designed with two bolts (Fig 2.4c), which failed in shear when the mass displacement reached the MR damper stroke. Unfortunately, the building was not instrumented during the earthquake.

After the earthquake, the building remained fully operative and there was no structural or significant non-structural damage despite its important flexibility. By looking at traces left on the swivels from which the TM is suspended, the relative displacement of the TM could be roughly estimated in the range of 30 through 100 cm. As shown in Fig, 3.1a, simulations of the building with the MR damper in passive state (off-state) up to the point of shearing-off, and by using as input an earthquake record recorded in rock at 3.7 km from the building site (Cerro Calán record), TM displacements are in the same range as observed above. Shown at the right side of the Figure is the estimated Y-direction roof displacement.

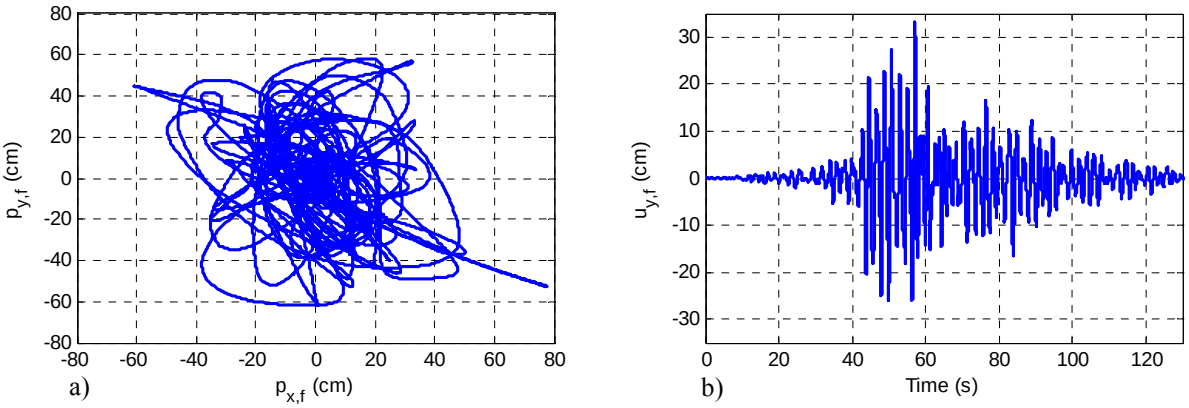

Figure 3.1. Simulation of building for the Cerro Calán record (Chile, 2010) using a model with measured periods: a) relative TM displacement, and b) roof building displacement along flexible edge

4. DEVELOPMENT OF FULLSCALE- MR DAMPER AND BUILDING IMPLEMENTATION

The new phase of this research includes the design, development, manufacturing, testing, and implementation of a real scale ±100 cm stroke MR damper with a maximum capacity of 400 kN, capable of controlling the TM along the flexible edge of the building in the Y-direction (Fig. 2.1). The new proposed concept is presented in Fig. 4.1 with a schematic view of the TM-MR assembly. Given the large stroke of ±100 cm, the length of the damper at mid stroke is 6.3 m. The MR damper will be connected below the TM at the centre of the mass. The design phase included also other options, such as that of a damper of ±20 cm stroke and higher capacity, but required an additional transmission system with displacement reductions of 1:5. The long-stroke damper solution was selected due to cost reasons, implementation robustness, and clearer understanding by the non-technical community. Indeed, the long-stroke damper has some disadvantages in comparison to a short-stroke solution in terms of manufacturing and testing.

The new long-stroke MR damper follows essentially the same internal design as the previous proof-of-concept device, but includes the following minor changes: i) seals were improved to hold fluid at high pressure and velocity; ii) the cable entry to the coils was modified to avoid fluid leakage; and iii) the gap-size and the coil protection were slightly modified to obtain a higher off-state viscous force. In the case of a full-scale implementation, a higher off-state force is relevant to get sufficient damping in the TM-MR assembly to be effective in case the control system fails. All these changes were first tried on the proof-of-concept MR damper previously described (150kN, ±10 cm stroke) which was tested again with two different MR- and one viscous fluid. These results will be presented in (Zemp. 2012)

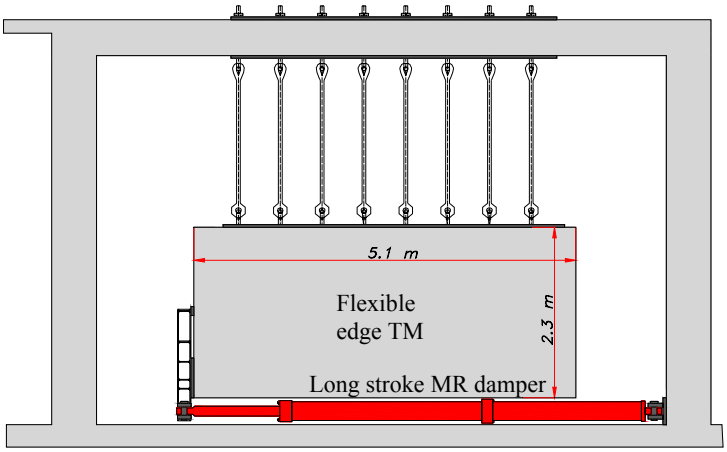

Figure 4.1. Sketch of long stroke MR damper connected to flexible edge TM

Because of the large velocities and long-stroke required to test the ±100 cm device as close as possible to real-life conditions, a significant improvement of the test rig was required to provide such velocities and stroke. The new test setup shown in Fig. 4.2 consists of a variable kinematic transmission with velocity rates 1:1 up to 1:9. The 400 kN long-stroke MR damper is mounted on top of the rig, while the 1000 kN hydraulic actuator is connected to the bottom end of the pivoting beam. Force and displacement are measured directly on the rod of the MR damper.

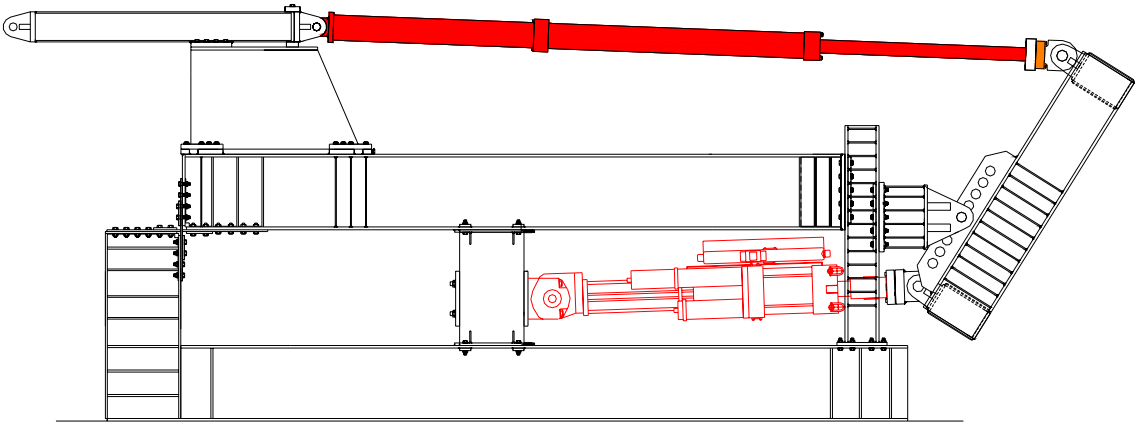

Figure 4.2. New test setup with kinematic transmission ratio up to 1:9 and MR damper in full stroke position

The physical controller with the push-back control option will be selected to steer the MR damper force. This requires that real time signals providing the sign of the damper force and the sign of the first mode displacement of the building are available. Some improvements proposed into the new system include that the sign of the MR damper force will be measured directly by a load cell built-in the damper, and not by relative velocities between the TM and the 21st floor. Please notice that the constitutive relationship of the MR damper shows that the sign of damper velocity and the sign of damper force do not coincide as the direction of velocity changes. Secondly, the sign of the displacement of the first mode in the building cannot be measured with velocity transducers or accelerometers, since their signals need to be integrated and filtered in real time to get reliable building displacements, leading to a delay of the signal. This delay cannot be compensated in a real earthquake case as we did for the pull-back tests in the proof-of-concept case. Delays become too large (approximately 0.1 – 0.4 s) to get adequate MR damper control performance during an earthquake. Consequently, a new reliable low-cost Real Time Structural Measurement procedure (RTSM) to detect building displacements is proposed next.

The general idea of RTSM is presented in Fig. 4.3a. A stiff string is installed between the basement

and the point of the structure where the displacement of the structure needs to be measured in real time. In the case of a high-rise building, such a line could be implemented in an elevator shaft. As the structure sways, the angle of the line φ is measured by a sensor, which could be an inclinometer or a laser sensor. Because the length of the string is known, the relative displacement between the points where the string is installed is provided in real-time (Zemp and De la Llera. 2012). Shown in Fig. 4.3b is the shaking table test setup implemented to prove the concept in a building model subjected to different ground motions; shown in Fig. 4.3c are some of the results obtained. The measured displacement (blue line) by the string tracks well the building displacement measured by a laser sensor (red line), and may be used reliably as control signal in the feed back loop. Please recall that for the physical controller, only the sign of the building displacement is of interest. For the real building implementation, the angle φ will be measured by a laser sensor to improve the RTSM even further.

As with any physical system identification, if the string is attached to a point where a mode has a zero crossing, the signal will filter the contribution of such mode leading to a better feedback signal in the case in which only the first mode displacement is of interest (Fig. 4.3a). This will be implemented in the TM-MR damper setup in building PA because the first mode displacement will be used as the real time control signal. In a real building implementation, a stiff string material is chosen to get high vibration frequencies in the string, and thus minimize the noise introduced by the string vibrations. Simulations of the string working in building PA, and measurements of frequency and damping of a real scale string will be published in (Zemp. 2012).

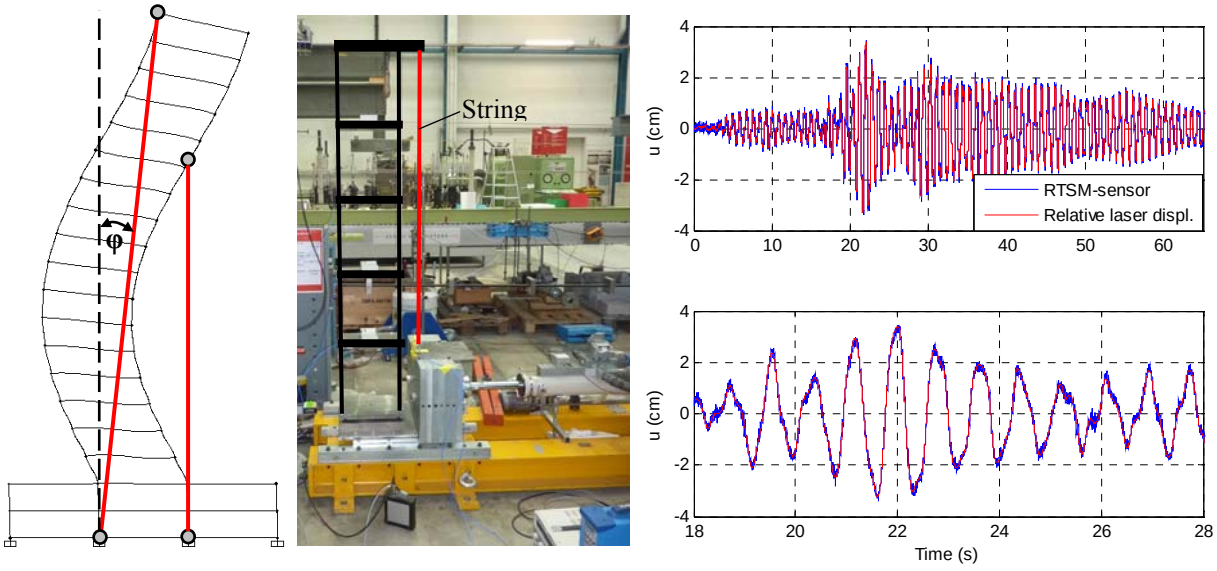

Figure 4.3. RTSM: a) Sketch of building setup (second mode deformation), b) Image of RTSM scaled shaking table test; c) Results of shaking table test for scaled Melipilla record, whole record on top, zoom on bottom

The planed real-scale implementation of the MR damper in the building includes a power source capable of preventing an important delay (less than 0.07s) in the response of the damper caused by the sudden change needed in current intensity and the relatively high coil inductance of about 2.0 H (Henry). The system considers a real time control of the MR damper by a PLC, which will acquire the real time data and control the ±120V power source to make the MR damper force track the logic of the physical controller.

A parametric analysis was performed using numerical simulation of the protected building PA using some of the newly available earthquake records of the 2010, Chile earthquake. Compared in Table 4.1 are the peak and RMS roof-displacement reductions with respect to the building without TMs. Three cases of the equipped building with bare TMs, with TMs connected to viscous dampers, and with TMs connected to our large-stroke MR damper, are presented. The table contains results of simulations of the structure for the cases with nominal and measured building periods. In assessing the magnitude of

the results, it is important to ponder that the total weight of the two TMs is only 1.19% of the mass associated with the first building mode. Reduction values range from zero (or even small increases in some cases) and up to 47%. Results are relevant not only for structural damage control but also because tolerance for no structural damage dropped drastically after the 2010 earthquake. It is apparent from the table that the MR damper solution improves the performance of the bare TMs and the TMs with viscous dampers. As expected, the solution with bare TMs works well only for some earthquake records and especially so when the TM period is well tuned with the first period of the building (nominal case). Viscous dampers improve this performance, and the solution with semi-active MR dampers improves it further. Please note that the MR solution leads to a significant improvement relative to the viscous and the bare TM case, when there is lack of tuning between the mass and the building (measured periods). This trend is also evident by comparing the standard deviations of the different cases.

Table 4.1. Peak and *(RMS)* reductions of building roof displacement (%)

	Earthquake records					
	S. Felipe 1985	Melipilla 1985	Llolleo 1985	Antumapu 2010	Conce. 2010	Mean.
Bare TMs, nominal periods	11 *(-2)*	32 *(24)*	10 *(-18)*	14 *(0)*	18 *(24)*	17 *(6)*
Bare TMs, measured periods	-16 *(-4)*	9 *(-11)*	-1 *(-11)*	-1 *(-8)*	-10 *(-2)*	-4 *(-7)*
	Standard Deviation.1.97 *(1.97)*					7 *(-1)*
TMs+2 VD, nominal periods	14 *(27)*	19 *(39)*	11 *(21)*	17 *(32)*	29 *(43)*	18 *(32)*
TMs+2 VD, measured periods	0 *(11)*	9 *(11)*	7 *(7)*	11 *(7)*	2 *(12)*	6 *(10)*
	Standard Deviation 0.68 (1.77)					12 (21)
TMs+2 MRD, nominal periods	20 *(34)*	23 *(44)*	14 *(26)*	23 *(38)*	32 *(47)*	22 *(38)*
TMs+2 MRD, measured periods	10 *(24)*	20 *(27)*	14 *(21)*	13 *(18)*	9 *(26)*	13 *(23)*
	Standard Deviation 0.51 *(1.00)*					18 *(31)*

5. COSTS AND EFECTIVNESS OF DIFRENT TM-SETUPS

MR dampers are an infinite collection of viscous dampers and conceptually very appealing for their real-time capacity of active selection of the most appropriate damping value. This apparent advantage also brings associated an extra cost of the dampers. In the building PA case presented, the cost of a MR damper is about 70% higher than the cost of a viscous damper of the same capacity. The higher cost of a MR damper is due essentially to the 10^2 higher cost of the MR-fluid in comparison to a conventional viscous fluid. To this cost we should add the value of damper control and the real-time signal acquisition system.

Nevertheless, a simple cost analysis for the solutions are presented in Table 5.1 for the cases of bare TMs, and the TMs with viscous and MR dampers. The solution considers a single damper on each TM to control both masses and, hence, the building in its most flexible Y-direction. It can be seen for this case that the costs of the viscous and MR dampers are about 22% and 44% higher, respectively, than the implementation of the bare TMs. Moreover, the third column of the table shows the overall mean reduction of each system. These mean values are extracted from the performance values presented in Table 4.1, and obtained as an overall mean value for the nominal and measured building period values and the peak and RMS displacements. The fourth column of Table 5.1 shows the normalized cost factor *f*, which is obtained as the ratio between the cost per square meter of net area and the overall displacement reduction factor. From this perspective, the MR-solution is clearly the most cost efficient solution. Saying this alternatively, one percentage point of reduction in building displacement has the lowest cost in the MR damper case. This result motivated the real-scale implementation of the long-stroke MR damper introduced earlier.

Table 5.1. Comparison of cost efficiency of different seismic protection configurations cases with bare TMs and with viscous and MR dampers

	Cost per m^2 of net area (USD)	Mean displacement reduction (%)	$f = \frac{\text{(Cost per } m^2\text{)}}{\text{(Mean disp. reduction)}}$
Bare TMs	12.6	3	5.54
TMs+VDs	15.4	16	1.17
TMs+MRDs	18.2	24	1.00

Another very interesting technical advantage of the MR damper over the VD solution is related to the outstanding capacity of the MR fluid to better absorb heating by the micro (iron) particles. Increasing of the internal pressure of the damper and decreasing of the viscosity of the fluid, as a result of the dissipated hysteretic work, is much less in the case of the MR damper in comparison to the VD. These results are explained in detail in (Zemp. 2012).

AKCNOWLEDGEMENT

This research was sponsored by Fondecyt Grant #1110377, and partially by Fondef Grant #D07I1006. The Ph.D. work of the first author has been sponsored by CONICYT through Grant #57090131 and by MECESUP through Grant #0710. The authors are grateful for this support and the technical support of Empa, Swiss Federal Laboratories for Materials Science and Technology.

REFERENCES

Zemp, R., De la Llera, J.C. and Breschi, L. (2008). Pendular tuned mass dampers in free-plan chilean tall buildings. *14th World Conference on Earthquake Engineering.* **11-0124**

Zemp, R., De la Llera, J.C. and Almazán, J.L. (2011). Tall building vibration control using a TM-MR damper assembly. *Earthquake Engineering & Structural Dynamics*. **Vol 40:** 339-354

Zemp, R., De la Llera, J.C. and Roschke, P. (2011). Tall building vibration control using a TM-MR damper assembly: Experimental results and implementation. *Earthquake Engineering & Structural Dynamics*. **Vol 40:** 257-171

Spencer, B.F. and Nagarajaiah, S. (2003). State of the art of structural control. *Journal of Structural Engineering.* **Vol 129**: 854-856.

Fujitani, H., et al. (2003). Development of 400kN magnetorheological damper for a real base-isolated building. *Proc. SPIE Conference 5052, 265.*

Weber, F., Feltrin, G., and Huth, O. (2006) Guidelines for structural control. *SAMCO final report*

Lee, H., Jung, H., Moon, S., Lee, S., Park, E. and Min, K. (2008). Experimental investigation of semiactive control systems based on MR dampers using full-scale steel frame building structure. *International Congress on Sound and Vibration, Daejeon, Korea*. 299-306.

Lin, P.Y., Chung, L.L. and Loh, C.H. (2005). Semiactive control of building structures with semiactive tuned mass damper. *Computer-aided Civil and Infrastructure Engineering***. Vol 20**: 35-51.

Dyke, S.J. and Spencer, B.F. (1996). Seismic response control using multiple MR dampers. *Proceeding 2nd Int. Workshop on Structura,l Control Hong Kong.* 163–173.

Yang, G., (2001). Large-scale magnetorheological fluid damper for vibration mitigation: modeling, testing and control. *Ph.D. Dissertation, Department of Civil Engineering and Geological Sciences, Notre Dame, Indiana, USA.*

Zemp, R. (2012). Modleing, design and implementation of a real scale MR damper. *PhD thesis in progress*

Zemp, R., De la Llera, J.C (2012). Real time structural measurement (RTSM) for active and semi-active feedback control devices. *Patent pending.*